

## ADSORPTION BEHAVIOUR OF THE *ARECA CATECHU* HUSK ULTRASONIC ASSISTED-PHOSPHORIC ACID ACTIVATED CARBON ON METHYLENE BLUE DYE

Nurul Iffah Mohd Said<sup>1</sup>, Siti Nur Najwa Arman<sup>1</sup>, Mohd Fauzi Abdullah<sup>1\*</sup>

<sup>1</sup>Faculty of Applied Sciences, Universiti Teknologi MARA (UiTM), Cawangan Perlis, Kampus Arau, 02600 Arau, Perlis, Malaysia

\*Corresponding author: mohdfauziabd@uitm.edu.my

### Abstract

The production of activated carbon from agricultural waste is one of the most environmental-friendly solutions by converting agricultural waste into valuable material. In this study, *Areca catechu* husk is converted into activated carbon to remove methylene blue (MB) dye in aqueous solution. This *Areca Catechu* husk was impregnated with phosphoric acid ( $H_3PO_4$ ) in an ultrasonic bath for 30 minutes to activate a pore surface before undergo carbonization at temperature of 700 °C for 2 hours. The physicochemical properties of the *Areca catechu* husk activated carbon was characterized by ash content, moisture content, bulk density, and iodine number. The result thus far shows that this activated carbon has low bulk density, low ash content and high iodine number that is very suitable for adsorption applications. The batch adsorption studies of MB dye were affected by adsorbent dosage, contact time, and initial concentration. The optimum parameters for the methylene blue adsorption were at adsorbent dosage of 0.06 g, initial concentration of 200 mg/L, and contact time of 180 minutes. According to the results of  $pH_{pzc}$  and batch adsorption study, this *Areca catechu* husk activated carbon is suitable to remove cation dyes such as MB in neutral and alkaline solution. Therefore, activated carbon of *Areca catechu* husk can be produced inexpensively as the demand from commercial activated carbon market for adsorption of dye in water.

**Keywords:** *Areca catechu* husk, activated carbon, ultrasonic-assisted phosphoric acid activation, adsorption behavior, methylene blue

Article History:- Received: 8 December 2024; Revised: 29 January 2025; Accepted: 5 February 2025; Published: 30 April 2025

© by Universiti Teknologi MARA, Cawangan Negeri Sembilan, 2025, e-ISSN: 2289-6368

DOI: 10.24191/joa.v13i1.4586

### Introduction

In the textile industry, dyes are highly useful substances that provide color and value to textiles, yarns, polymers, and other substrates. The most commonly used dyes in the textile industry are basic, reactive, and acid dyes. Basic dyes like methylene blue (MB) have chromophores with positive ions and amino groups that give off a strong color. Most of the time, the MB is used to color cotton and silk (Khodaie et al., 2013; Olusakin et al., 2022). Due to its high resistance to light, heat, and reducing agents, MB is hard to break down or get rid of from aqueous solution. Various method has been investigated to remove this MB dye from water such as, adsorption process (Bansal and Goyal, 2005), chemical coagulation/flocculation (Wang et al., 2007), biological degradation (Crini at al., 2007), reverse osmosis (Avlonitis et al., 2008), ozonation (Wu et al., 2008), membrane-filtration (Saleh and Gupta, 2012), ion exchange (Gupta et al., 2012), photo-catalytic (Saravanan et al., 2013), oxidation process (Saravanan et al., 2014), and electro-chemical process (Ali, 2018). However, each removal technique has drawbacks. Amongst all treatments, adsorption seems to be the excellent removal technique due to its simple design, sludge-free operation, and high efficiency in dye removal (Baidya & Kumar, 2021). A most promising material used in the adsorption technique is an activated carbon. Activated carbon is widely utilized in industry as an adsorbent for liquid and gas purification and

separation, as well as a catalyst and catalytic support that apply to the elimination of colors, aromas, tastes, and pollutants in water purification and other detoxification procedures (Joshi et al., 2021). Commercial activated carbon is typically derived from natural minerals, such as wood or coal, and is considered costly (Yahya et al., 2015). The primary obstacle encountered in the realm of commercial manufacturing lies in attempting to generate activated carbon at a cost-effective rate (Husien et al., 2022). In the present scenario, it is evident that biomass utilization for producing activated carbon emerges as the most appropriate alternative. Preparations of activated carbon from biomass have many advantages. The precursors are diverse, low-cost, abundant, and renewable (Hamad & Idrus, 2022). Activated carbon from biomass precursors shows excellent surface properties with a high degree of porosity and a high specific surface area. Further, the utilization of waste biomass to produce activated carbon contributes to decreasing costs of waste disposal and the negative impact on the environment (Gayathiri et al., 2022).

One of the most abundance crop in Malaysia is Pinang Merah, the scientific name is *Areca catechu*. This plant is commonly known as areca palm or areca nut palm (betel palm), found in parts of east Africa, Asia, and much of tropical Pacific. It is grown commercially for its seed crop which is the areca nut and can be found in India, Bangladesh, Taiwan and other Asian countries. Traditionally, Areca nut is a main ingredient for chewing (eat together with petal leaf), which is believed to be native to Sri Lanka, West Malaysia and Melanesia (IARC, 1985). The husk is the outer part of areca fruit enclosed by a fibre in the middle layer of husk and it can be obtained via dehusking or by manual stripping. Areca nut husk fibre contains 53.2 % cellulose, 32.9% hemicellulose and 7.2% lignin (Hassan et al., 2010). Cellulose could be used as an adsorbent due to its good mechanical properties, non-toxic and easy disposability after use (Suhas et al., 2016). The husk is nearly 15 – 30% of the raw areca nut and often regarded as worthless and either burnt inefficient or wasted. Although the husk of areca nuts can be employed as an adsorbent, this kind of agricultural waste has a very poor adsorption capability. (Baidya & Kumar, 2021). Therefore, their adsorption capability must be increased by activation, which can be achieved chemically or physically and assisted with ultrasonication or microwave irradiation.

Ultrasonic extraction is a method for preparing carbonaceous compounds from biomass, producing high-purity microporous, mesoporous, and multistage porous carbonaceous products with a large specific surface area (Sajjadi et al., 2019; Chen et al., 2020). Applying ultrasound in carbonization and activation improves problems of low specific surface area and single pore structure. Undoubtedly, materials featuring a multi-phase pore structure and a modifiable micropore/mesopore ratio can be effectively processed through this ultrasonic treatment (Wang et al., 2022). Interestingly, ultrasonic-assisted chemical activation utilize lower temperature process, which can be done at room temperature with 20 – 40 kHz ultrasonic frequency instead of physical activation (temperatures ranges between 800 and 1000 °C in the presence of oxidizing gases or its mixture of gases such as CO<sub>2</sub>, air, and steam) (Swiatkowski, 2008). In addition, the ultrasonic-assisted chemical activation also leads to a high yield of activated carbon production (Bora et al., 2021).

Therefore, this study aims to converted a waste biomass of *Areca catechu* husk into activated carbon by ultrasonic assisted chemical activation using phosphoric acid as activating agent. The prepared activated carbon was characterized by its physicochemical properties such as a bulk density, ash content, iodine test, point-of-zero-charge (pH<sub>pzc</sub>) analysis and Fourier Transform Infrared (FTIR). The adsorption performance of the activated carbon was done by determine the MB colour removal on the effect of adsorbent dosage, initial dye concentration, and contact time, respectively.

## Methods

### Preparation of Activated Carbon

The *Areca catechu* samples were gathered from a plantation area in Universiti Teknologi MARA (UiTM) Perlis branch. After dehusking, the husk was ground into smaller pieces, about 12 to 15 mm, and then repeatedly rinsed with distilled water to get rid of all the pollutants, dirt, and dust. Then, the husk was dried in the oven for 24 hours at 100 °C to remove the moisture content. After cooling, the dried husk was ground again and sieved through a 425 µm screen. The sample was impregnated with

80% H<sub>3</sub>PO<sub>4</sub> (ratio 1:1) in ultrasonic bath for 30 minutes. Then, it was placed in a lid-covered crucible and carbonized at 700 °C for 2 hours in a furnace. The sample was taken and washed with hot distilled water (4 times) to remove any excess acid to neutralize the sample, and then kept in oven at 110°C for 12 hours. After cooling, *Areca catechu* husk activated carbon (labelled as ACHAC) was kept in an air-tight bottle and placed in a desiccator for further use.

### Characterization of The Activated Carbon

The ACHAC was characterized in terms of the physicochemical properties such as bulk density, ash content, iodine number, and point-of-zero-charge (pH<sub>pzc</sub>) analysis. The functional groups analysis was done by Fourier transform infrared (FTIR) spectroscopy.

#### Bulk density

The bulk density of the prepared activated carbon was obtained according to the ASTM D2854 by measuring the volume of distilled water displaced by a known mass of the experimentally produced activated carbon sample using a measuring cylinder. For this experiment, 0.5 g of ACHAC was filled in 1 mL volume of 10 mL cylinder. The bulk density then calculated as follow:

$$\text{Bulk density} = \frac{W_c}{V_c} \quad (1)$$

Where W<sub>c</sub> (g) is the weight of dried activated carbon and V<sub>c</sub> (mL) is cylinder volume packed with dried activated carbon.

#### Ash content

In this experiment, the ash content was determined based on the standard ASTM D2866 method using a muffle furnace. The sample was heated in the muffle furnace at 650 °C for 3 hours. Then, the crucible was cooled to ambient temperature and weighed. The percentage of ash was calculated as follow:

$$\text{Ash (\%)} = \frac{W_{s3} - W_{s2}}{W_{s1}} \times 100 \quad (2)$$

Where W<sub>s3</sub> (g) is the weight of crucible containing ash, W<sub>s2</sub> (g) is the weight of crucible, and W<sub>s1</sub> (g) is the weight of original activated carbon use.

#### Iodine test

The iodine number indicates the micro-porosity of activated carbon and defined as the milligram of iodine absorbed per g of carbon. Following the standard method iodine number ASTM D4607-94, HCl solution (5 wt%: 5 mL) was added to dried activated carbon (1 g) and allowed to boil. After cooling the solution, iodine solution (10 mL: 0.1N) was added and shaken vigorously for 30 seconds, filtered, and washed with distilled water. The whole filtrate was titrated against 0.1 N sodium thiosulphate using starch as an indicator. The iodine number is determined using equation (3).

$$\text{Iodine number} = \frac{\text{Weight of iodine adsorbed on carbon (mg)}}{\text{Weight of carbon (g)}} \quad (3)$$

#### pH at point zero of charge (pH<sub>pzc</sub>)

The pH<sub>pzc</sub> was determined according to the method described in our recent study (Abdullah & Othman, 2023). The experiment was conducted in a 250 mL conical flask which was filled with 50 mL of 0.01 M NaCl for different initial pH. The initial pH of the NaCl solution ranges from pH 2 to 11 and was adjusted by using 0.1 HCl and 0.1 M NaOH. Then, 0.1 g of ACHAC was added to each conical flask with a different initial pH (pH2 – pH10). The flask was sealed and shaken for 24 hours at 150 rpm using an orbital shaker. After that, the final pH of each sample was taken. The value of pH<sub>pzc</sub> for ACHAC was determined by plotting the graph between the initial pH (pH<sub>i</sub>) and final pH (pH<sub>f</sub>) against the pH value.

**Fourier Transform Infra-Red Spectroscopy (FTIR) analysis**

FTIR analysis was used to determine the existence of functional group of ACHAC before and after adsorption of MB dye solution. For the preparation of the pellet, 0.1 g KBr was mixed with 0.002 g of ACHAC before and after the adsorption of MB dye solution, respectively. After that, the mixture hydraulically was pressed at 850 psi to obtain a thin transparent disk. Then, the thin disk was placed in an oven at 100 °C for 24 hours to prevent interference with existing water vapor. The pellet was placed in a PerkinElmer Frontier FTIR Spectroscopy and scanned 32 times for 2 minutes with a data spacing of 1.929 cm<sup>-1</sup> and a resolution of 4 cm<sup>-1</sup>. The shifted peaks of ACHAC before and after adsorption was compared within the scanning ranges of 4000 to 400 cm<sup>-1</sup>.

**Adsorption Batch Experiment**

MB dye stock solution 1000 mg/L was prepared by dissolving 1.0 gram of MB in 1 L of distilled water. MB solution for batch adsorption experiments was prepared by diluted the stock solution into desired concentrations. Three parameters that affect the adsorption process were investigated (i.e. the adsorbent dosage (0.02 – 0.1 g/L), the contact time (60 – 240 min), and the initial concentration of the MB dye (25 – 300 mg/L). The pH and the temperature were fixed at 7 and 30 °C throughout the experiment. The respective sample was mixed in a 250-mL conical flask and placed on the hot plate with a stirrer and agitated at 90 rpm. The solution was filtered and analyzed using a UV-visible spectrophotometer (Shimadzu UV-1001) at a wavelength of 662 nm to determine the final concentration. The percentage of MB colour removal for all the batch adsorption experiments was calculated using equation (4). After the adsorption, all the residual ACHAC were collected and washed with distilled water under constant stirring three times, and then dried at 100 °C for 24 hours. This dry adsorbed ACHAC was applied in the FTIR-analysis.

$$\text{Colour removal (\%)} = \frac{(\text{Initial concentration} - \text{Final concentration})}{\text{Initial concentration}} \times 100 \tag{4}$$

**Result and Discussion**

**Characterization of The Activated Carbon**

**Bulk density**

The determination of bulk density is a valuable indicator to determine the ability to float characteristics of the adsorbent material. It was observed that when the activated carbon is introduced into the water, a foul odour is detected, which indicates that the activated carbon has the potential to yield favourable adsorption outcomes and establish improved interaction with the adsorbates. The observation of a higher value in bulk density suggests that the activated carbon exhibits lower porosity and compaction (Durrani et al., 2022). According to the data presented in the Table 1, it is evident that ACHAC exhibits a relatively low bulk density, measuring at 0.23 g/ml indicating that the activated carbon exhibits notable characteristics of high carbon porosity and compaction. The value of bulk density can also be attributed to random arrangement of micro-crystallites and with strong cross-linking which produce porous structure (Christian et al., 2017).

Table 1. Physicochemical properties of ACHAC

Properties	Value
Bulk density, g/mL	0.23
Ash content, %	2.43
Iodine value, mg/g	1226.06

Table 2. Comparison of phosphoric acid activated carbon obtained from this work and other reports

Description	This work	Patnukao & Pavasant (2008)	Nedjai et al. (2021)	Joshi et al. (2021)	Daniel et al. (2023)
Raw material	<i>Areca catechu</i> husk	<i>Eucalyptus</i> bark	Baobab fruit shell	<i>Areca catechu</i> nut	<i>A. erioloba</i> seed pods
Activation	Ultrasonic, 30 min, room temp.	Stirred, 3 min, room temp.	Stirred, 1 hr, 50 °C	Stirred, 1 hr, room temp.	Room temp. overnight
Carbonization	700 °C, 2 hr		500 °C, 1 hr	400 °C, 2 hr	500 °C, 1 hr
Bulk density, g/mL	0.23	500 °C, 1 hr 0.25	0.3	-	-
Ash content, %	2.43	4.88	17.7	-	24.01
Iodine value, mg/g	1226.06	1043	1248.35	888	662

### Ash content

The analysis of ash content is a widely used to determine the residual mineral content after removing water and organic matter through a heating process. Ash refers to non-carbonaceous or mineral substances that do not undergo chemical bonding with carbonaceous surfaces. The composition of activated carbon includes a variety of undesirable mineral substances, which are significant as they must not be destroyed during the heating process. A high ash content is unwanted for activated carbon because it decreases the mechanical strength of the activated carbon and consequently impacts its adsorption capacity (Abdullah et al., 2001; Maulina & Iriansyah, 2018). According to the data presented in Table 1 and comparison study in Table 2, it can be observed that ACHAC exhibits a relatively low content (2.43%). This finding suggested that ACHAC shows a significant mechanical strength, contributing to its excellent adsorption capacity (Patnukao & Pavasant, 2008). Moreover, the ash content of ACHAC was within the commercially acceptable value (< 5%) (Liew et al, 2018). These properties are important since higher ash content (> 5 wt%) could have catalytic effect that can lead to undesired reaction (e.g. catalytic cracking reactions between metal oxides in the ash with the other compounds in the activated carbon) occurred during the high temperature (Dizbay-Onat et al., 2017).

### Iodine number

Iodine number, also called iodine adsorption, is thought to be one of the best ways to figure out how well activated carbon can absorb things and how good it is. It is often used because it is easy and quick to do. The higher the iodine number, the more likely it is that activated carbon has a very big micropore structure and a lot of surface area for adsorption (Ektepe et al., 2017; Du et al., 2021). The iodine value was employed to estimate the microporosity and mesoporosity of the prepared activated carbon. The iodine number of ACHAC is presented in Table 1 illustrates the value is 1226.06 mg/g. A comparison of iodine value in Table 2 illustrates a comparable iodine number with study by Nedjai et al (2021) but higher than the others. Increasing the carbonization temperature also affect the porosity of the activated carbon, at which as carbonization temperature increases, the porosity also increases due to the release of tars from the cross-linked framework generated by phosphoric acid treatment (Joshi et al., 2021). In addition, a high value of iodine number obtained by ACHAC might be due to the assistance of ultrasonic during activation, in which a multi-phase pore structure and a modifiable micropore/mesopore ratio can be effectively processed through ultrasonic treatment (Wang et al., 2022). Hence, the higher value of iodine number in this study recommended that the ultrasonic-assisted H<sub>3</sub>PO<sub>4</sub> activation has highly affected the microporosity and mesoporosity of the ACHAC, thus possibly enhancing the adsorption capacity of MB dye.

### Point of zero charge (pH<sub>pzc</sub>) analysis

The study of pH<sub>pzc</sub> was significant as it aimed to determine the surface charge characteristics of the adsorbent material. A comparative analysis was conducted by plotting a graph illustrating the disparity

between the initial and final pH values, with the initial pH serving as the independent variable (Kosmulski, 2020). When the pH of a solution is lower than the pH at  $pH_{pzc}$ , it results in the adsorbent's surface acquiring a positive charge. The decrease in adsorption capacity can be attributed to the elevated concentration of  $H^+$  ions present on the surface of the adsorbent (Bardhan et al., 2020). This increased concentration leads to a competitive interaction with the cationic MB dye for available binding sites. When the pH of a dye solution exceeds the  $pH_{pzc}$ , it results in the surface of the adsorbent material acquiring a negative charge (Daniel et al., 2023). The enhanced adsorption capacity can be attributed to the presence of a negatively charged adsorbent, which exhibits a strong affinity towards cationic dyes.

The  $pH_{pzc}$  value of ACHAC was obtained at 4.9 (indicated by red-cross in Figure 1). This value indicates that ACHAC surface may gain a positive charge when pH is less than  $pH_{pzc}$ . Therefore, it does not favor the adsorption of cationic MB dye. Conversely, when the pH of the dye solution increases ( $pH > pH_{pzc}$ ), the ACHAC surface becomes negatively charged indicating that cationic MB dye can be adsorbed onto ACHAC. Hence, electrostatic forces are generated from the attraction between the reactive groups (negatively charged) of ACHAC and MB dye (positively charged) (Jawad et al., 2022).

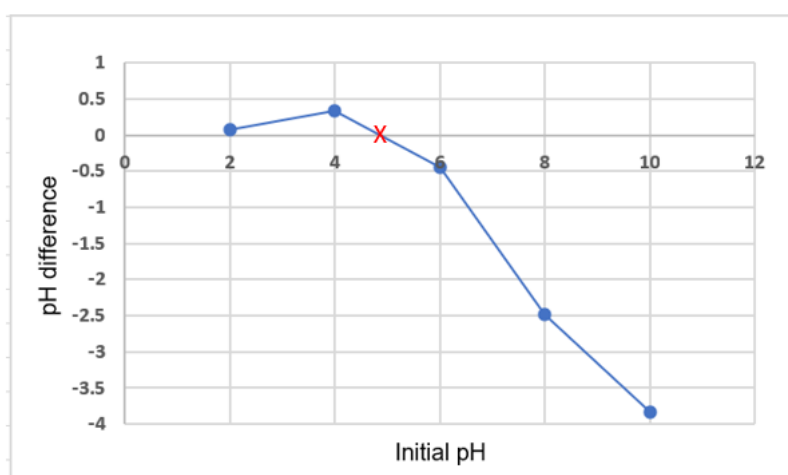


Figure 1. Determination of Point of Zero Charge ( $pH_{pzc}$ )

### FTIR analysis

Figure 2 demonstrates the FTIR spectrum of the ACHAC before adsorption (a) and after adsorption (b) of MB dye. The broad peak depicted at  $3444.36\text{ cm}^{-1}$  before MB adsorption and at  $3400.50\text{ cm}^{-1}$  after MB adsorption reflects to O-H stretching vibration of hydroxyl groups indicating the presence of active functional groups on activated carbon surface (Haghbin & Shahrak, 2021). The band in range  $3200\text{--}3650\text{ cm}^{-1}$  have also attributed to the hydrogen-bonded O-H group of alcohol and phenol (Reddy et al., 2012). The peaks located at  $2925.4\text{ cm}^{-1}$  and  $2924\text{ cm}^{-1}$  are corresponds to the C-H stretching vibration (Wibawa et al., 2020). The band at  $1647\text{ cm}^{-1}$  before the adsorption of MB and the band at  $1567.9\text{ cm}^{-1}$  after the adsorption of MB were assigned to C=C stretching in a cyclic alkene. The band at  $1396.4\text{ cm}^{-1}$  before adsorption and  $1375.4\text{ cm}^{-1}$  after adsorption of MB, respectively may correspond to O-H stretching bending in the alcohol group (Joshi et al., 2021).

The peak appeared between  $1000\text{--}1250\text{ cm}^{-1}$ , yielding the fingerprint of this ACHAC. The absorption band at  $1073.3\text{ cm}^{-1}$  before adsorption and  $1072\text{ cm}^{-1}$  after adsorption have been described as either Si-O or C-O stretching in alcohol, ether, or hydroxyl group (Hussain et al., 2023). Lastly, the absorption peak at around  $500\text{ cm}^{-1}$  shows the stretch function of PO confirming  $H_3PO_4$  impregnation on the surface of the adsorbent (Kassahun et al., 2022; Dimbo et al., 2024). The MB dye adsorbed on the ACHAC surface was confirmed by the shifting of a tiny peak around  $1100\text{ cm}^{-1}$  and the emergence of bands around  $800\text{ cm}^{-1}$  which pertain to N-H out of plane bending vibration and stretching vibration of  $-CH_2$ , respectively (Shang et al., 2015; Jawad et al., 2022). The appearance, diminishing and shifting of various surface groups portrays by FTIR analysis showed that the MB has been successfully adsorbed on the ACHACH.

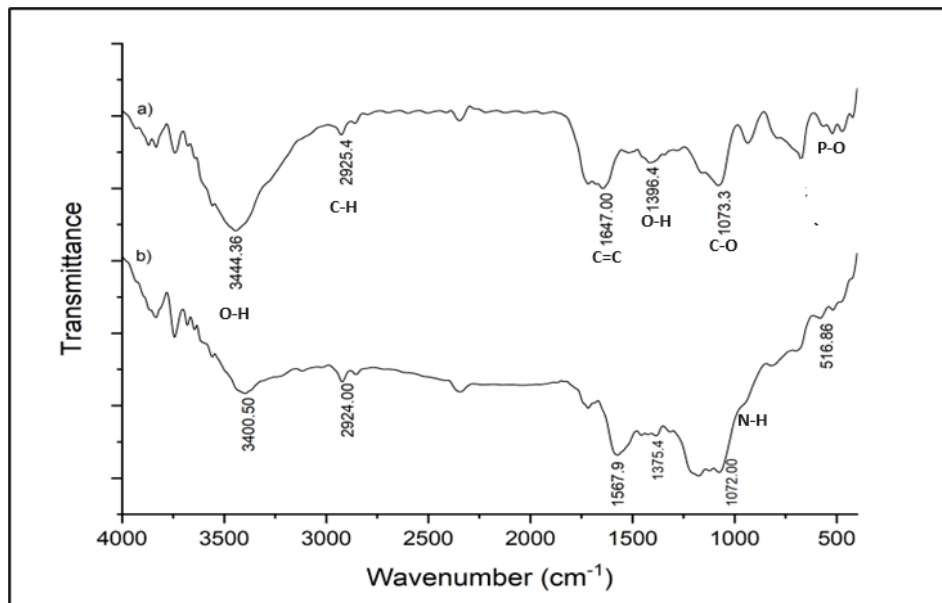


Figure 2. FTIR analysis of ACHAC (a) before and (b) after adsorption of MB dye

### Adsorption Batch Study

Adsorption studies experiment was conducted to examine adsorption behaviour of ACHAC on removal capacity of MB dye at different adsorption conditions (i.e. adsorbent dosage, initial concentration of MB and adsorbent contact time).

### Effect of adsorbent dosage

Figure 3 shows the percentage of colour removal by various of ACHAC dosage. The figure illustrates that when the dosage of adsorbent is increased from 0.02 g to 0.06 g, the percentage of colour removal increases from 57.9% to 92.6%. This may be because the adsorbent's surface area has increased, increasing the number of binding sites that are accessible for the adsorption process (Badessa et al., 2020). The increase in adsorbent dosage will increase availability of active adsorption sites, thus increasing in effective surface area for adsorption (Gupta et al., 2022). Apparently, the percentage of colour removal decreased insignificantly after reached maximum dosage at 0.06 g due to the saturation of the binding sites (Baloo et al., 2021). Furthermore, increasing the adsorbent dose while maintaining a constant MB concentration will increase the surface area of the adsorbent as well as the accessibility and availability of adsorption sites for dye molecules, leading to instauration in the adsorbent sites (Ali et al., 2022).

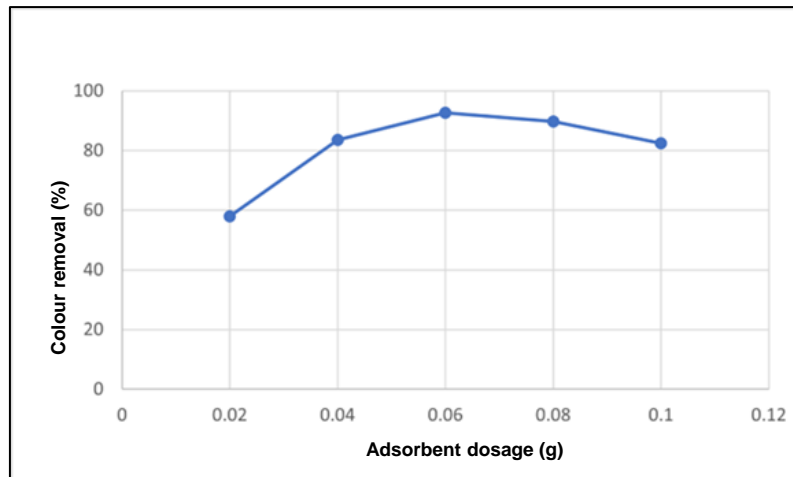


Figure 3. Effect of adsorbent dosage  
(Condition: Concentration 100 mg/L, pH 7, temp. 30 °C and contact time 120 min.)

### Effect of contact time

Effect of contact time can influence the economic efficiency of the process and the adsorption of kinetics. The extent to which carbon can absorb dye is primarily influenced by the availability of binding sites, with many of these sites being present initially. Consequently, the dye exhibits a high affinity for these readily accessible sites. Over time, there has been a noticeable decline in the availability of vacant spaces. This leads to a saturation point where the carbon surface reaches its maximum capacity and stopped to absorb any additional dye molecules (Basrur & Ishwara, 2019). Figure 4 display that the MB colour removal increases from 65.8% to 88.4% when the contact time increase from 60 min to 180 min, which might be due to more vacant spaces available on ACHAC for MB adsorption. The result shows that the adsorption process is quick in the beginning and found to decrease with increase in contact time. In the beginning, sharp increase in the rate of adsorption is due to larger surface area and availability of vacant sites on the adsorbent. After reaching equilibrium time, repulsive force between the adsorbate and the adsorbent lead to the decrement of adsorption capacity (Basrur & Ishwara, 2019). The similar findings were also reported by numerous studies of adsorption of MB on a variety of adsorbents (Nasrullah et al., 2018; Alamin et al., 2021; Durrani et al., 2022).

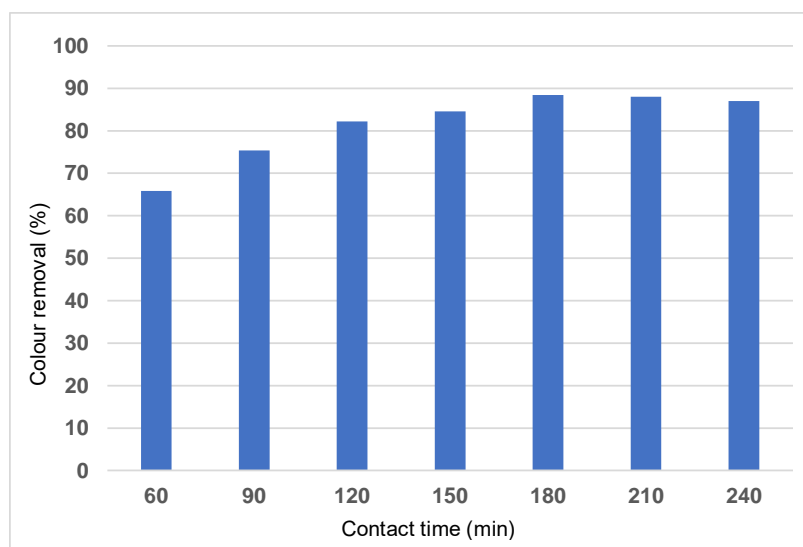


Figure 4. Effect of contact time  
(Condition: 0.06 g dosage, Concentration 100 mg/L, pH 7, & temp. 30 °C)

### Effect of MB concentration

The amount of concentration of MB plays important role in adsorption capacity of activated carbon. The effect of methylene blue concentration was determined at different concentrations of methylene blue solutions. Figure 5 shows that, the colour removal was increase from 72.4% until 98.4%. The maximum percentage of MB removal was obtained at MB concentration of 200 mg/L. The adsorption capacity increase but remain constant after achieved equilibrium. Thus, as the initial dye concentration increases, the collision rate between MB dye and GL-HAC surface also increases resulting in more MB cations being transferred to the GL-HAC surface. This happened when the concentration of dye solution increased, the collision rates of dyes ions and adsorbent increase (Ramli et al., 2022). This effect develops a strong driving force for dye molecules to overcome the mass transfer resistance between aqueous and solid phases (Jawad et al., 2016). Generally, as the amount of initial concentration of MB dye increases, the adsorption capacity decreases. At high concentrations of MB limits, the vacancy of bidding sites decrease thus reduces the amount of methylene blue removal (Ahmed et al., 2019).

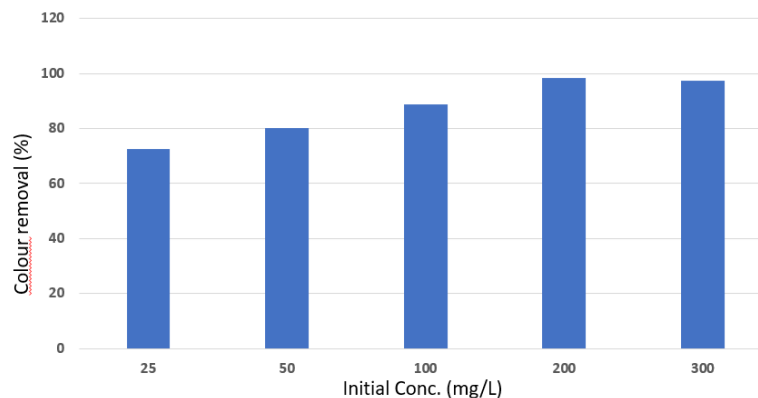


Figure 5. Effect of initial MB dye concentration  
(Condition: 0.06 g dosage, pH 7, temp. 30 °C, & 180 minutes contact time)

### Conclusion

ACHAC was successfully prepared by ultrasonic-assisted  $H_3PO_4$  activation with fast preparation. The physicochemical properties of prepared ACHAC showed that ACHAC has low bulk analysis, low ash content and higher iodine number. Batch adsorption experiments of ACHAC with MB dye aqueous solution were done and the optimum adsorption condition of different parameters like adsorbent dose, initial concentration and contact time as 0.06 g/L, 200 mg/L and 180 min. The appearance, diminishing and shifting of various surface groups portrays by FTIR analysis showed that the MB has been successfully adsorbed on the ACHAC. The results of this study suggested that ACHAC might be a potential adsorbent for the effective removal of synthetic cationic dyes from water.

### Acknowledgement

Highly gratitude to the Staff of Instrumental Laboratory, UiTM Perlis Branch in preparing and conditioning the analytical instruments used in this study. The author(s) received no financial support for the research.

### Author Contribution

MF Abdullah – Supervision, Writing – review & editing; Nurul Iffah – Formal Analysis, Data curation,; Nur Najwa – Methodology, Investigation

### Conflict of Interest

Authors declare no conflict of interest.

### References

Abdullah, M. F., & Othman, N. F. (2023). Physicochemical and Adsorption Properties of Guava Leaves-Activated Carbon by Hydrochloric Acid on Adsorption of Methylene Blue. *Scientific Research Journal*, 20(1), 33-49. <https://doi.org/10.24191/srj.v20i1.20669>

- Abdullah A. H., Kassim, A., Zainal, Z., Mohd Zobir, H., Kuang, D., Wooi, S. O., & Ahmad, F. (2001). Preparation and characterization of activated carbon from Gelam wood bark (*Melaleuca cajuputi*) *Malaysian Journal of Analytical Sciences.*, 7, 65-68.
- Ahmed, M. H., Okoye, P. U., Hummadi, E., & Hameed, B. (2019). High-performance porous biochar from the pyrolysis of natural and renewable seaweed (*Gelidiella acerosa*) and its application for the adsorption of methylene blue. *Bioresource Technology*, 278, 159–164. <https://doi.org/10.1016/j.biortech.2019.01.054>
- Alamin, N. U., Khan, A. S., Nasrullah, A., Iqbal, J., Ullah, Z., Din, I. U., ... & Khan, S. Z. (2021). Activated carbon-alginate beads impregnated with surfactant as sustainable adsorbent for efficient removal of methylene blue. *International journal of biological macromolecules*, 176, 233-243. <https://doi.org/10.1016/j.ijbiomac.2021.02.017>
- Ali, I. (2018). Microwave assisted economic synthesis of multi walled carbon nanotubes for arsenic species removal in water: batch and column operations. *Journal of Molecular Liquids*, 271, 677–685. <https://doi.org/10.1016/j.molliq.2018.09.021>.
- Ali, J., Bakhsh, E. M., Hussain, N., & Bilal, M., Akhtar, K., Fagieh, T. M, Danish, E. Y., Asiri, A. M., Su, X., & Khan, S. B. (2022). A new biosource for synthesis of activated carbon and its potential use for removal of methylene blue and eriochrome black T from aqueous solutions. *Industrial Crops and Products*. 179. <https://doi.org/10.1016/j.indcrop.2022.114676>
- Avlonitis, S. A., Poullos, I., Sotiriou, D., Pappas, M., & Moutesidis, K. (2008). Simulated cotton dye effluents treatment and reuse by nanofiltration. *Desalination*, 221, 259–267. <https://doi.org/10.1016/j.desal.2007.01.082>.
- Badessa, T. S., Wakuma, E., Yimer, A. M., & Yimer, A. M. (2020). Bio-sorption for effective removal of chromium (VI) from wastewater using moringa stenopetala seed powder (MSSP) and banana peel powder (BPP), *BMC chemistry*, 14(1):71. <https://bmchem.biomedcentral.com/articles/10.1186/s13065-020-00724-z>
- Baidya, K. S., & Kumar, U. (2021). Adsorption of brilliant green dye from aqueous solution onto chemically modified areca nut husk, *South African Journal of Chemical Engineering*, 35, 33-43. <https://doi.org/10.1016/j.sajce.2020.11.001>.
- Baloo, L., Isa, M. H., Sapari, N. B., Jagaba, A. H., Wei, L. J., Yavari, S., Razali, R., & Vasu, R. (2021). Adsorptive removal of methylene blue and acid orange 10 dyes from aqueous solutions using oil palmwastes-derived activated carbons. *Alexandria Engineering Journal*, 60, 5611–5629. <https://doi.org/10.1016/j.aej.2021.04.044>
- Bansal, R.C., & Goyal, M., (2005). *Activated Carbon Adsorption*. CRC press, New York. <https://doi.org/10.1201/9781420028812>.
- Bardhan, M., Novera, T. M., Tabassum, M., Islam, M. A., Jawad, A. H., & Islam, M. A. (2020). Adsorption of methylene blue onto betel nut husk-based activated carbon prepared by sodium hydroxide activation process. *Water Science and Technology*, 82(9), 1932–1949. <https://doi.org/10.2166/wst.2020.451>
- Basrur D., & Ishwara Bhat J. (2019). An investigation on the characterization of activated carbon from areca leaves and their adsorption nature towards different dyes. *Global Nest Journal*, 21(2), 124–130. <https://doi.org/10.30955/gnj.002877>
- Bora, M., Benoy, S. M., Tamuly, J., & Saikia, B. K. (2021). Ultrasonic-assisted chemical synthesis of activated carbon from low-quality subbituminous coal and its preliminary evaluation towards supercapacitor applications. *Journal of Environmental Chemical Engineering*, 9(1), 104986. <https://doi.org/10.1016/j.jece.2020.104986>

Burakov, A. E., Galunin, E. V., Burakova, I. V., Kucherova, A. E., Agarwal, S., Tkachev, A. G., & Gupta, V. K. (2018). Adsorption of heavy metals on conventional and nanostructured materials for wastewater treatment purposes: A review. *Ecotoxicology and environmental safety*, 148, 702-712. <https://doi.org/10.1016/j.ecoenv.2017.11.034>

Chen, F.; Ji, Y.; Deng, Y.; Ren, F.; Tan, S.; Wang, Z. (2020). Ultrasonic-assisted fabrication of porous carbon materials derived from agricultural waste for solid-state supercapacitors. *J. Mater. Sci.* 55(22), 11512–11523. <https://link.springer.com/article/10.1007/s10853-020-04751-y>

Christian, N. S., Manga, N. H., Raoul, T. T. D., & Gabche, A. S., (2017). Optimisation of Activated Carbon Preparation by Chemical Activation of Ayous Sawdust, Cucurbitaceae Peelings and Hen Egg Shells Using Response Surface Methodology. *International Research Journal of Pure and Applied Chemistry*. 14. 1-12. 10.9734/IRJPAC/2017/36021.

Crini, G., Peindy, H., Gimbert, F., Robert, C., (2007). Removal of C.I. Basic Green 4 (Malachite Green) from aqueous solutions by adsorption using cyclodextrin-based adsorbent: kinetic and equilibrium studies. *Separation and Purification Technology* 53(1), 97–110. <http://dx.doi.org/10.1016/j.seppur.2006.06.018>

Daniel, L. S., Rahman, A., Ndakola, H. M., Kapolo, P., & Jonnalagadda, S. B. (2023). Preparation and characterisation of activated carbon derived from *Acacia erioloba* seed pods by chemical activation with phosphoric acid. *Water Science and Technology*. Preprints. <https://doi.org/10.20944/preprints202302.0409.v1>

Dimbo, D., Abewaa, M., Adino, E., Mengistu, A., Takele, T., Oro, A., & Rangaraju, R. (2024). Methylene blue adsorption from aqueous solution using activated carbon of *spathodea campanulate*, *Results in Engineering*, 21, 101910. <https://doi.org/10.1016/j.rineng.2024.101910>.

Dizbay-Onat, M., Vaidya, U.K., Lungu, C.T., (2017). Preparation of industrial sisal fiber waste derived activated carbon by chemical activation and effects of carbonization parameters on surface characteristics. *Industrial Crops and Products*, 95, 583–590. <https://doi.org/10.1016/j.indcrop.2016.11.016>

Du, C., Liu, B., Hu, J., & Li, H. (2021). Determination of iodine number of activated carbon by the method of ultraviolet-visible spectroscopy. *Materials Letters*, 285, 129-137. <https://doi.org/10.1016/j.matlet.2020.129137>

Durrani, W., Nasrullah, A., Khan, A., Fagieh, T. M., Bakhsh, E. M., Akhtar, K., Khan, S. B., Din, I. U., Khan, M. S., & Bokhari, A. (2022). Adsorption efficiency of date palm based activated carbon-alginate membrane for methylene blue. *Chemosphere*, 302, 134793. <https://doi.org/10.1016/j.chemosphere.2022.134793>

Ekpete, O. A., Marcus, A. C., & Osi, V. (2017). Preparation and Characterization of Activated Carbon Obtained from Plantain (*Musa paradisiaca*) Fruit Stem. *Journal of Chemistry*, 2017, 1–6. <https://doi.org/10.1155/2017/8635615>

Fito, J., Abewaa, M., Mengistu, A., Angassa, K., Ambaye, A. D., Moyo, W., & Nkambule, T. T. (2023). Adsorption of methylene blue from textile industrial wastewater using activated carbon developed from Rumex abyssinicus plant. *Scientific Reports*, 13(1). <https://doi.org/10.1038/s41598-023-32341-w>

Gayathiri, M., Pulingam, T., Lee, K. S., & Sudesh, K. (2022). Activated carbon from biomass waste precursors: Factors affecting production and adsorption mechanism. *Chemosphere*, 294, 133764. <https://doi.org/10.1016/j.chemosphere.2022.133764>

Gupta, S., Vishesh, Y., Sarvshrestha, N., Bhardwaj, A. S., Kumar, A., Topare, N. S., Raut-Jadhav, S., Bokil, S. A., & Asiri, A. M. (2022). Adsorption isotherm studies of Methylene blue using activated carbon of waste fruit peel as an adsorbent. *Materials Today: Proceedings*, 57, 1500–1508. <https://doi.org/10.1016/j.matpr.2021.12.044>

Gupta, V. K., Ali, I., Saleh, T. A., Siddiqui, M. N., Agarwal, S., (2012). Chromium removal from water by activated carbon developed from waste rubber tires. *Environmental Science and Pollution Research*, 20, 1261–1268. <https://doi.org/10.1007/s11356-012-0950-9>

Gupta, V. K., Kumar, R., Nayak, A., Saleh, T. A., & Barakat, M. A. (2013). Adsorptive removal of dyes from aqueous solution onto carbon nanotubes: a review. *Advances in colloid and interface science*, 193, 24-34. <https://doi.org/10.1016/j.cis.2013.03.003>

Hagbini, M. A., & Shahrak, M. N. (2021). Process conditions optimization for the fabrication of highly porous activated carbon from date palm bark wastes for removing pollutants from water. *Powder Technology*, 377, 890–899. <https://doi.org/10.1016/j.powtec.2020.09.051>

Hamad, H. N., & Idrus, S. (2022). Recent Developments in the Application of Bio-Waste-Derived Adsorbents for the Removal of Methylene Blue from Wastewater: A Review. *Polymers*, 14(4), 783. <https://doi.org/10.3390/polym14040783>

Hassan, M. M., Wagner, M. H., Zaman, H. U. & Khan, M. A. (2010) Physico-Mechanical Performance of Hybrid Betel Nut (*Areca catechu*) Short Fiber/Seaweed Polypropylene Composite, *Journal of Natural Fibers*, 7:3, 165-177. <https://doi.org/10.1080/15440478.2010.504394>

Hussain, O. A., Hathout, A. S., Abdel-Mobdy, Y. E., Rashed, M., Rahim, E. A., & Fouzy, A. (2023). Preparation and characterization of activated carbon from agricultural wastes and their ability to remove chlorpyrifos from water. *Toxicology Reports*, 10, 146–154. <https://doi.org/10.1016/j.toxrep.2023.01.011>

Husien, S., El-Taweel, R. M., Salim, A. I., Fahim, I. S., Said, L. A., & Radwan, A. G. (2022). Review of activated carbon adsorbent material for textile dyes removal: Preparation, and modelling. *Current Research in Green and Sustainable Chemistry*, 5, 100325. <https://doi.org/10.1016/j.crgsc.2022.100325>

IARC (1985). *IARC Monographs on the Evaluation of the Carcinogenic Risk of Chemicals to Humans*, Vol. 37, *Tobacco Habits Other than Smoking; Betel-Quid and Areca-nut Chewing; and Some Related Nitrosamines*, Lyon, IARC Press.

Jawad, A. H., Mamat, N.F.H., Abdullah, M. F. and Ismail, K. (2016). Adsorption of methylene blue onto acid-treated mango peels: Kinetic, equilibrium and thermodynamic. *Desalination and Water Treatment*, 59, 210–219. <http://dx.doi.org/10.5004/dwt.2017.0097>

Jawad, A. H., Saber, S. E. M., Abdulhameed, A. S., Reghioia, A., AlOthman, Z. A., & Wilson, L. D. (2022). Mesoporous activated carbon from mangosteen (*Garcinia mangostana*) peels by H<sub>3</sub>PO<sub>4</sub> assisted microwave: Optimization, characterization, and adsorption mechanism for methylene blue dye removal. *Diamond and Related Materials*, 129, 109389. <http://dx.doi.org/10.1016/j.diamond.2022.109389>

Joshi, S., Shrestha, R. G., Pradhananga, R. R., Ariga, K., & Shrestha, L. K. (2021). High Surface Area Nanoporous Activated Carbons Materials from Areca catechu Nut with Excellent Iodine and Methylene Blue Adsorption. *J. of Carbon Research*, 8(1), 2. <https://doi.org/10.3390/c8010002>

Kassahun, E., Fito, J., Tibebe, S., Nkambule, T. T., Tadesse, T., Sime, T., & Kloos, H. (2022). The application of the activated carbon from cordia africana leaves for adsorption of chromium (III) from an aqueous solution. *Journal of Chemistry*, 2022, 1-11. <http://dx.doi.org/10.1155/2022/4874502>

Khodaie, M., Ghasemi, N., Moradi, B., & Rahimi, M. (2013). Removal of methylene blue from wastewater by adsorption onto ZnCl<sub>2</sub> activated corn husk carbon equilibrium studies. *Journal of Chemistry*, 2013, 383985. <https://doi.org/10.1155/2013/383985>

Kosmulski, M. (2020). The pH dependent surface charging and points of zero charge. *VIII. Update Advances in Colloid and Interface Science*, 275, 102064. <https://doi.org/10.1016/j.cis.2019.102064>

- Liew, R. K., Azwar, E., Peter, N. Y. Y., Lim, X. y., Cheng, C. K., Jo-Han, N., Jusoh, A., Lam, W. H., Ibrahim, M. D., Ma, N. L., & Lam, S. S. (2018). Microwave pyrolysis with KOH/NaOH mixture activation: A new approach to produce micro-mesoporous activated carbon for textile dye adsorption, *Bioresource Technology*, 266, 1-10. <https://doi.org/10.1016/j.biortech.2018.06.051>.
- Maulina, S., & Iriansyah, M. (2018). Characteristics of activated carbon resulted from pyrolysis of the oil palm fronds powder. *IOP Conference Series*, 309, 012072. <https://doi.org/10.1088/1757-899x/309/1/012072>
- Nedjai, R., Al-Khatib, M. a. F. R., Alam, M. Z., & Kabbashi, N. A. (2021). Adsorption of Methylene Blue onto Activated Carbon developed from Baobab fruit shell by Chemical Activation: Kinetic Equilibrium Studies. *IJUM Engineering Journal*, 22(2), 31–49. <https://doi.org/10.31436/iiumej.v22i2.1682>
- Nasrullah, A., Bhat, A. H., Naeem, A., Isa, M. H., & Danish, M. (2018). High surface area mesoporous activated carbon-alginate beads for efficient removal of methylene blue. *International journal of biological macromolecules*, 107, 1792-1799. <https://doi.org/10.1016/j.ijbiomac.2017.10.045>
- Olusakin, P., Oladiran, T., Oyinkansola, E. & Joel, O. (2022). Results in engineering Methylene blue dye: Toxicity and potential elimination technology from wastewater. *Results Eng.*, 16, 100678. <https://doi.org/10.1016/j.rineng.2022.100678>
- Patel, R. K., Prasad, R., Shankar, R., Khare, P., & Yadav, M. (2021). Adsorptive removal of methylene blue dye from soapnut shell & pineapple waste derived activated carbon. *International Journal of Engineering & Science Technology*, 13(1), 81–87. <http://dx.doi.org/10.4314/ijest.v13i1.12S>
- Patnukao, P., & Pavasant, P. (2008). Activated carbon from *Eucalyptus camaldulensis* Dehn bark using phosphoric acid activation, *Bioresource Technology*, 99 (17), 8540-8543, <https://doi.org/10.1016/j.biortech.2006.10.049>.
- Ramli, M. R., Shoparwe, N. F., & Ahmad, M. S. (2022). Methylene Blue Removal Using Activated Carbon Adsorbent from Jengkol Peel: Kinetic and Mass Transfer Studies. *Arabian Journal for Science and Engineering*, 48, 8585-8594. <https://doi.org/10.1007/s13369-022-07141-5>
- Reddy, K. S. K., Al Shoaibi, A., & Srinivasakannan, C. (2012). A comparison of microstructure and adsorption characteristics of activated carbons by CO<sub>2</sub> and H<sub>3</sub>PO<sub>4</sub> activation from date palm pits. *New Carbon Materials*, 27(5), 344–351. [https://doi.org/10.1016/s1872-5805\(12\)60020-1](https://doi.org/10.1016/s1872-5805(12)60020-1)
- Sajjadi, B.; Chen, W.Y.; Egiebor, N.O. A. (2019). Comprehensive review on physical activation of biochar for energy and environmental applications. *Rev. Chem. Eng.* 35, 735–776. <https://doi.org/10.1515/revce-2017-0113>
- Saleh, T.A., & Gupta, V. K., (2012). Synthesis and characterization of alumina nano-particles polyamide membrane with enhanced flux rejection performance. *Separation & Purification Technology*, 89, 245–251. <https://doi.org/10.1016/j.seppur.2012.01.039>.
- Saravanan, R., Joicy, S., Gupta, V. K., Narayanan, V., & Stephen, A., (2013). Visible light induced degradation of methylene blue using CeO<sub>2</sub>/V<sub>2</sub>O<sub>5</sub> and CeO<sub>2</sub>/CuO catalysts. *Materials Science and Engineering: C.*, 33 (8), 4725–4731. <https://doi.org/10.1016/j.msec.2013.07.034>
- Saravanan, R., Gupta, V. K., Narayanan, V., & Stephen, A., (2014). Visible light degradation of textile effluent using novel catalyst ZnO/γ-Mn<sub>2</sub>O<sub>3</sub>. *J. Taiwan Institute of Chemical Engineers*, 45, 1910–1917. <https://doi.org/10.1016/j.jtice.2013.12.021>.
- Shang, H., Lu, Y., Zhao, F., Chao, C., Zhang, B., & Zhang, H. (2015). Preparing high surface area porous carbon from biomass by carbonization in a molten salt medium, *RSC Advances*, 5 (92), 75728–75734.

Swiatkowski, A. (1999). Industrial carbon adsorbents, *Stud. Surf. Sci. Catal.* 120, 69–94. [https://doi.org/10.1016/S0167-2991\(99\)80549-7](https://doi.org/10.1016/S0167-2991(99)80549-7)

Suhas, Gupta, V. K., Carrott, P.J.M., Singh, R., Chaudhary, M., & Kushwaha, S. (2016). Cellulose: a review as natural, modified and activated carbon adsorbent. *Bioresour. Technol.* 216, 1066–1076. <https://doi.org/10.1016/j.biortech.2016.05.106>.

Wang, J. P., Chen, Y. Z., Ge, X. W., Yu, H. Q., (2007). Optimization of coagulation–flocculation process for a paper-recycling wastewater treatment using response surface methodology. *Colloids and Surfaces A: Physicochemical and Engineering Aspects*, 302, 204–210. <https://doi.org/10.1016/j.colsurfa.2007.02.023>.

Wang, J., Li, W., Zhao, Z., Musoke, F. S. N., & Wu, X. (2022). Ultrasonic Activated Biochar and Its Removal of Harmful Substances in Environment. *Microorganisms*, 10(8), 1593. <https://doi.org/10.3390/microorganisms10081593>

Wu, J., Doan, H., & Upreti, S., (2008). Decolorization of aqueous textile reactive dye by ozone. *Chemical Engineering Journal*, 142, 156–160. <https://doi.org/10.1016/j.cej.2007.11.019>.

Wibawa, P. J., Nur, M., Asy'ari, M., & Nur, H. (2020). SEM, XRD and FTIR analyses of both ultrasonic and heat generated activated carbon black microstructures. *Heliyon*, 6(3), e03546. <https://doi.org/10.1016/j.heliyon.2020.e03546>

Yahya, A., Al-qodah, Z., & Ngah, C. W. Z. (2015). Agricultural bio-waste materials as potential sustainable precursors used for activated carbon production: A review. *Renewable and Sustainable Energy Reviews*, 46, 218–235. <https://doi.org/10.1016/j.rser.2015.02.051>